E3S Web of Conferences **95**, 01001 (2019) https://doi.org/10.1051/e3sconf/20199501001
ICPEME 2019

Machinability of SMART Forging Process Materials in Intermittent Cutting

2nd Report : Machinability in Normal Cutting Region and Selection of Optimum Cutting Condition

Mitsuaki Murata[1,*], *Makoto* Hino[2] , *Ryoichi* Kuwano[2] *and Syuhei* Kurokawa[3]

[1]Department of Machanical Engineering, Kyushu Sangyo University 2-1-3 Matsukadai, Higashi-ku, Fukuoka, 813-8503, Japan
[2]Department of Mechanical System Engineering, Hiroshima Institute of Technology, 2-1-1 Miyake, Saeki-ku, Hiroshima 731-5193 Japan
[3]Department of Mechanical Engineering, Kyushu University, 744 Motooka, Nishi-ku, Fukuoka, 819-0935 Japan

Abstract. Transmission used in automobiles is indispensable from the viewpoint of improvement of maximum speed, quietness and fuel consumption even if the power source of automobile is changed from internal combustion engine to electric motor in the future. We are studying a heat treatment process for imparting machinability to the forged material after hot forging used for a transmission of automobiles. In the past, the heat stored in the material after hot forging was merely released into the atmosphere. We succeeded in imparting machinability to the material by cooling while well controlling the heat stored in the forged material after hot forging. In the previous paper [1], we reported the progress of tool wear of this forged material in the high-speed cutting region with the cutting speed of 200 m/min or more in intermittent cutting. In this report, we conducted cutting experiments on the machinability of this developed forged material in the normal cutting speed region with the cutting speed less than 200 m/min. As a result, at the cutting speed V of V=157 m/min or less, it reached the conclusion that the built-up edges frequently occurred and the tool was chipped due to it. From the previous report and the results of this experiment, it was found that the cutting speed V of about V=213 m/min is optimum for cutting these forged materials with cemented carbide.

1 Introduction

Due to the depletion of fossil fuels and the impact of global warming caused by carbon dioxide emissions, electric vehicles (EV) will be mainstream in the future. This is also clear from the policy "To prohibit sales of gasoline and diesel vehicles by 2040 " that France set as a goal of the "Paris Agreement", an international framework for global warming countermeasures.

The electric motor, which is the drive source of the EV, generates the maximum torque from the beginning at the time of start-up. It has completely different characteristics of output torque from the internal combustion engine. Therefore, it is possible to drive in the required speed range by directly driving the driving wheels with the motor itself or a combination of the motor and speed reducer without using a clutch or a transmission which was necessary for an automobile using an internal combustion engine. Particularly, since the in-wheel type EV does not require a transaxle and a differential mechanism, its parts configuration changes considerably as compared with cars using internal combustion engines. However, for the reasons such as improvement of maximum speed, improvement of fuel economy, contribution to miniaturization of the motor, etc., the necessity of transmission in EV is sufficient even with the arrival of the EV era. The performance required for the EV transmission is required to have high rigidity to receive the force of the motor that outputs the maximum torque from the beginning at the time of starting as described above. In addition, the EV purchaser also considers the quietness of the car because the EV has no engine noise. Therefore, reduction of the noise emitted from the transmission which has been damped by the drive sound of the internal combustion engine is also a problem. Therefore, forged products made of chromium steel or chromium molybdenum steel used for power transmission gear shaft of automobile transmission such as main shaft, output shaft, counter gear etc. have the same demand as before even if the power source of the automobile shifts from an internal combustion engine to an electric motor. Because they are high toughness and have high machinability.

The transmission shaft material before gear cutting process is required to have various diameter parts in one shaft, it is manufactured by hot forging chromium steel or chromium molybdenum steel which are high toughness steel. Thereafter, in order to perform gear cutting at the outer peripheral portion, it is necessary to perform annealing or normalizing heat treatment for imparting machinability. Then, gear tooth is cut by hobbing machine or the like, and it is shipped as a product. We focused on the heat treatment process after forging and tried to be able to use heat applied by hot forging for

* Corresponding author: murata@ip.kyusan-u.ac.jp

annealing and normalizing process after forging. As a result, we succeeded in developing a forging process comparable to conventional forging methods and called "SMART forging process" [2], [3]. However, verification of the machinability between the material manufactured by the conventional forging method and the material manufactured by the SMART forging process has not been sufficiently verified yet. Comparison of machinability of materials manufactured by conventional forging and SMART forging processes has been studied mainly by comparison of cutting force by lathe turning. When comparing machinability of both materials by cutting force, there was no clear difference in the results. In other words, even if the heat treatment process after forging was changed, the machinability was about the same as that of the conventional method. However, as the result of the turning cut experiment in the high cutting speed region *V* of *V*=200 m / min to *V*=300 m / min, the cutting force of the material manufactured by the SMART forging process is smaller than that by the conventional method. Therefore, in the previous report, the progress of tool wear by the face milling tool were investigated in the high cutting speed region *V* of *V*=200 m / min or more. As a result, it was found that the material manufactured by the SMART forging process obviously has a longer tool life. We conducted the same experiment as in the previous report in the standard cutting condition region when cutting general steel materials with cemented carbide tool. As a result, it was found that the cutting tool frequently chipped in the general cutting condition region. We report the cause of the chipping and the optimum cutting conditions for these forged materials by observing the chips flowed from cutting.

2 Experimental Method and Materials

-A Materials

The SMART forging process which has been developed is the process for imparting machinability for gear cutting to the forged materials used for the power transmission gear shaft of automobile transmission such as main shaft, output shaft, counter gear etc made of chromium steel and chromium molybdenum steel which are high toughness steels shown in Fig. 1.

Figure 2 shows the forging process by a conventional method and the forging process by the SMART forging. In the conventional forging method, the material is heated to 1260 degrees Celsius before forging and forged. Then, in order to carry it out to the heat treatment step, once cooled to normal temperature and it is transported to the heat treatment plant. After that, in order to give the machinability to the forged material, annealing treatment is performed by reheating up to 900 degrees Celsius. and then cooling. On the other hand, in the SMART forging, it is the same as the conventional forging process to heat the material up to 1200 degrees Celsius in order to perform forging. It cools while controlling the heat that stored in the material after forging. By processing this method, it is possible to give the similar cutting machinability as the conventional forging process. As the result, superiority will be generated compared with the conventional forging method due to cooling, delivery time, energy associated with reheating energy, cost and CO2 emissions, etc.

Fig. 1. SMART forged products before gear cutting process

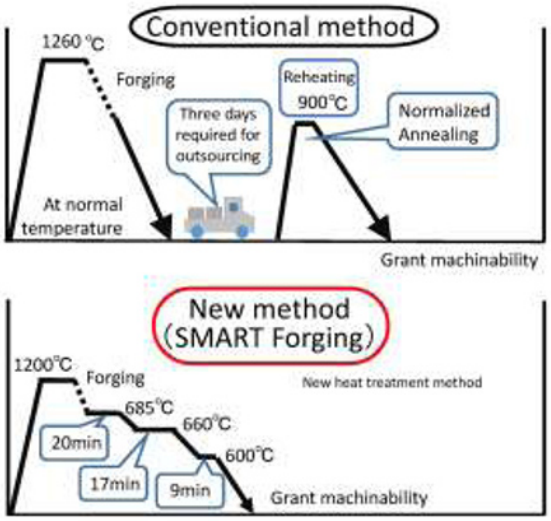

Fig. 2. Comparison between conventional forging process and the SMART forging process

The materials that used in this experiment are JIS high-toughness steel SCr20 and SCM420. They are the same lot as the material used in the previous report. And for each material, the total of four work materials were prepared, including forged to annealed material by the conventional construction method and the material that forged SMART forging method. The specifications of the material are shown in Table 1.

Hardness of the materials was measured by the Brinell hardness test because all of the workpieces used in the experiment were forged products. The end faces of each material were polished with a surface grinding machine. And after grinding, it measured 10 points and the average of 8 points excluding the maximum value and the minimum value was taken as the hardness of the material. The results are shown in fig. 3. From this result, it can be seen that the hardness of each material is almost constant.

Table 1. Specification of the materials (before forging)

JIS		SCr20	SCM420
ISO		20Cr4	– 18CrMO4 ⇕ 34CrMO4
Chemical composition (%)	Cr x100	115	110
	Mo x100	–	18
	C x100	21	22
	Si x100	24	31
	Mn x100	80	78

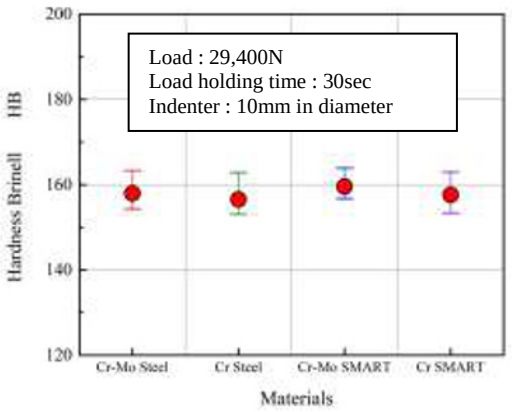

Fig. 3. Brinell hardness of each material

-B Experimental method of tool flank wear width

The experimental setup and experimental method are the same as those reported in the previous report. Details are shown below again. To compare the progress of tool flank wear during intermittent cutting by using milling machine to compare with the conventional forged materials and the SMART forged materials. An outline of the experimental apparatus is shown in fig. 4. The face mill diameter of 100mm is attached to the milling machine. And then, only one cutting edge is attached to this face mill and the end face of the material is cut. The reason why only one cutting edge was attached is that in the case of abrasion experiment with multiple cutting edges, when the front cutting edge of the measured cutting edge suffers sudden damages, the influence thereof will not affect the next edge. The cutting edge once cuts the end face of workpiece at the depth of cut t=1.0mm was regarded as one cutting cycle, and the tool flank face was observed with the CCD microscope shown in fig. 4 for each cycle and recorded the width of flank wear.

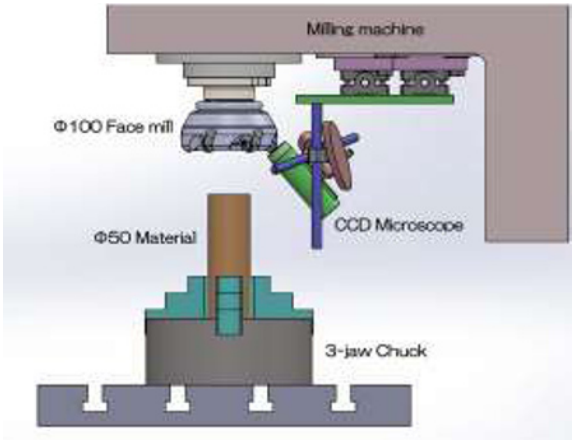

Fig. 4. Experimental set up of tool wear experiment

Table 2 shows the cutting conditions used in the experiment. The rotation speed of the main spindle is selected by the cutting speed V of V=100m/min to V=300m/min including standard cutting conditions for cutting steel materials with cemented carbide. As the result, the experiment was conducted at the cutting speed V of V=94m/min, V=157m/min, V=213m/min and V=308m/min. The feed amount per cutting edge f is f=0.1mm/edge, but it has to be used the value close to f=0.1 mm/edge at each cutting speed. The depth of cut t was set to t=1.0mm in both of the cutting speeds. If the cutting edge was chipping, the same experimental conditions were repeated several times to examine whether chipping was sudden or constant.

The cutting distance in one cycle is geometrically calculated from the diagram shown in fig. 5 and equation (1). From the fig. 5 and eq. (1), the cutting distance l_n for one cycle at each cutting speed is
l_n=23.3 m when V=94m/min, f=0.09mm/edge,
l_n=25.4 m when V=157m/min, f=0.08mm/edge,
l_n=16.9 m when V=213m/min, f=0.12mm/edge, and
l_n=23.6 m when V=308m/min, f=0.09mm/edge.

Table 2. Cutting conditions

Ex. Condition No.	No.1	No.2	No.3	No.4
Cutting tool	Φ100 Face mill with One cutting edge			
Cuttig speed	94.2m/min	157.0m/min	213.5m/min	307.9m/min
(Spindle rotarion)	(300min^{-1})	(500min^{-1})	(680min^{-1})	(980min^{-1})
Feed rate	0.09mm/edge	0.08mm/edge	0.12mm/edge	0.09mm/edge
(Table feed speed)	(27mm/min)	(40mm/min)	(82mm/min)	(88mm/min)
Depth of cut	1mm			

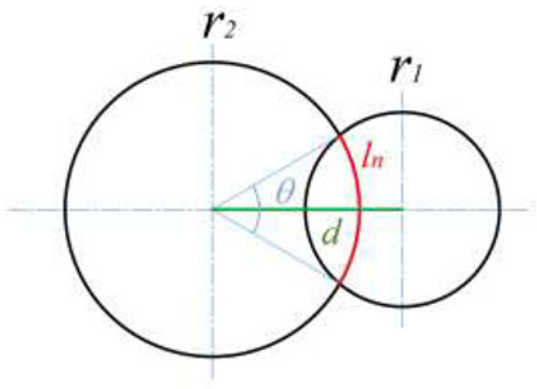

r_1 : Radius of material
r_2 : Radius of face mill
d : The center to center distance between tool and work
l_n : Cutting distance of one revolution

Fig. 5. Geometric diagram of cutting length

$$l = \sum_{k=0}^{n-1} \frac{\pi}{180} r_2^2 \cos^{-1}\left\{ \frac{\left(r_1 + r_2 - n\_f\right)^2 + r_2^2 - r_1^2}{r_1^2 + \left(r_1 + r_2 - n\_f\right)^2} \right\} \qquad (1)$$

-C Measurement of cutting temperature

The cutting temperature was compared by measuring the tool-work thermoelectromotive force. (E.M.F.) [4-7] Figure 6 shows the experimental setup. In cutting conditions, the cutting speed was V=409m/min in addition to previous cutting speed conditions shown in table 2. The feed rate of one cutting edge f was f=0.12mm/edge when V=409m/min and all depth of cut t was t=1.0mm. The cutting tool was same as the previous experiment. (100mm in diameter face mill attached only one cutting edge)

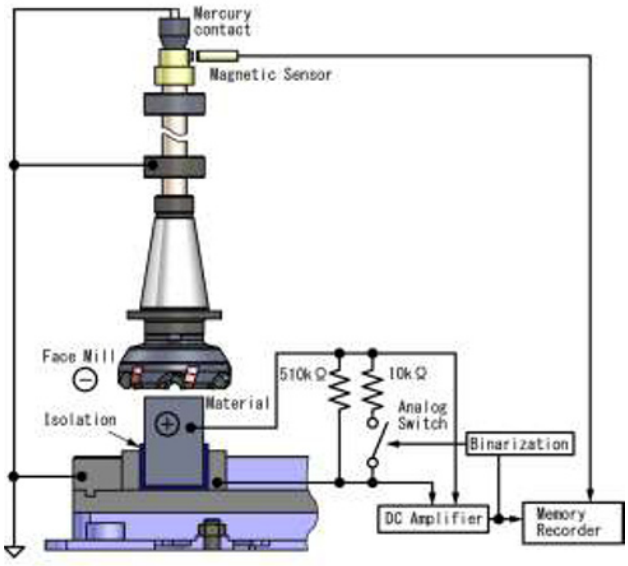

Fig. 6. Experimental set up of E.M.F. measurement

E.M.F. generated at the cutting tool and the workpiece interface is outputted from the mercury contact on the top of the spindle axis and the isolated workpiece. E.M.F is led to the DC amplifier and amplified by two hundredfold. Amplified E.M.F. is converted to the digital signal by the built-in A/D converter on the memory recorder and recorded with the proximity sensor signal output pulse per rotation. The method of digitizing the measured waveform is the same as in the previous report, so it is omitted in this paper.

3 Result and Discussion

The results of the tool wear experiment are shown in Fig.7. Figure 7-a shows the relationship between the cutting distance and the maximum flank wear width at the cutting speed V of V=94 m/min. The vertical axis of the graph shows the maximum flank wear width (mm) and the horizontal axis shows the cutting distance (m). For easy comparison, it is plotted the results with 4 different materials simultaneously in one figure. Cross marks in the graph indicate the points at which the experiment was stopped as the tool chipped during the experiment. Similarly, fig. 7-b shows the results at a cutting speed V of V=157 m/min, fig. 7-c shows the results at a cutting speed V of V=213 m/min, and fig. 7-d shows the results at a cutting speed of V=308 m/min. From these results, it can be seen that the tool immediately chips when these forged materials are cut in the normal cutting speed region when the steel material are cut by cemented carbide that were the purpose of this experiment. The conventional forged chrome molybdenum steel at the cutting speed V of V=157 m/min exceeds the maximum flank wear width of V_b=0.6 mm without causing chipping during the experiment. However, it can be said that it is highly probable that chipping did not happen by considering from the results with other materials. Regarding this, we plan to confirm additional experiments in the future.

In order to know the cause of chipping in this normal cutting speed region, examination of the chip thickness ratio and observation of the chip surface were carried out. The chip thickness ratio r is the ratio of the chip thickness to the depth of cut, and its value approaches 1 as the sharpness is better. And it can be obtained from equation (2). In eq. (2), t_o is the depth of cut, and t_c is the average thickness of the discharged chip.

$$r = \frac{t_o}{t_c} \qquad (2)$$

It can be seen from fig. 8 that the chip thickness ratio abruptly decreases from the cutting speed V of V=157 m/min to V=213 m/min and becomes the smallest at the cutting speed V of V=308 m/min. From the cutting speed V of V=94 m/min to V=157 m/min, the chip thickness ratio shows a very large value and it can be seen that the good chips are not discharged in this area.

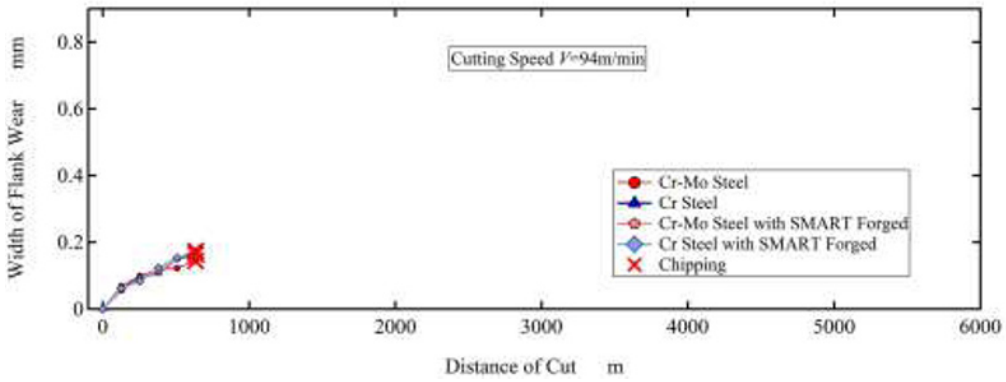

(a) Cutting speed *V*=94.2m/min

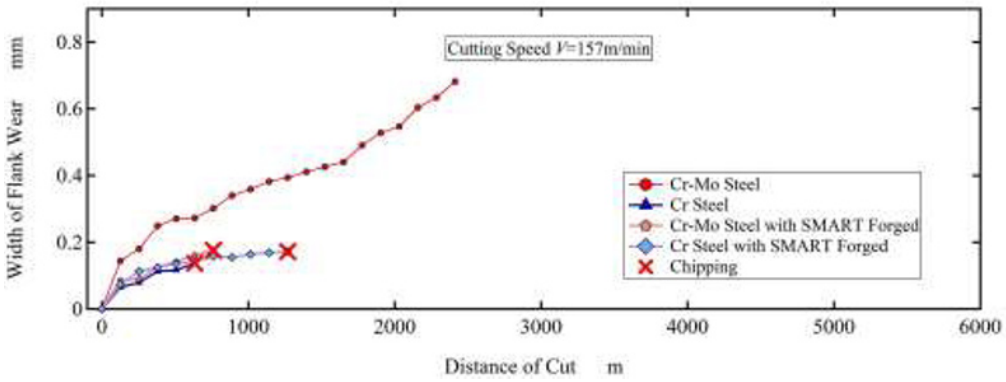

(b) Cutting speed *V*=157m/min

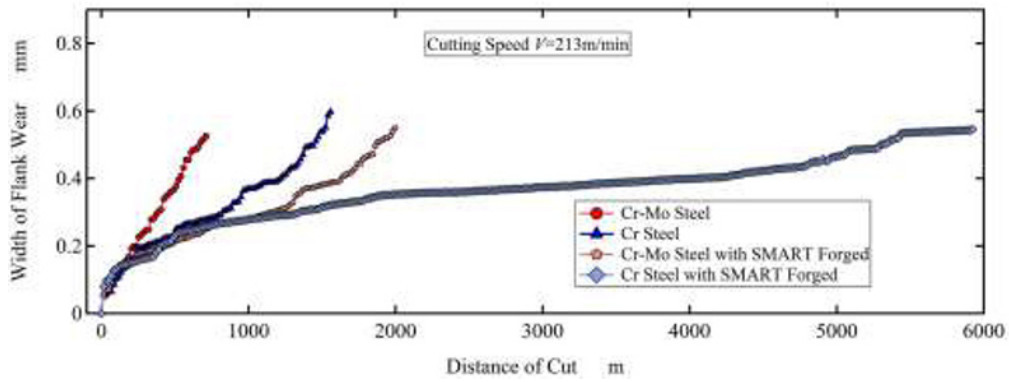

(c) Cutting speed *V*=213m/min

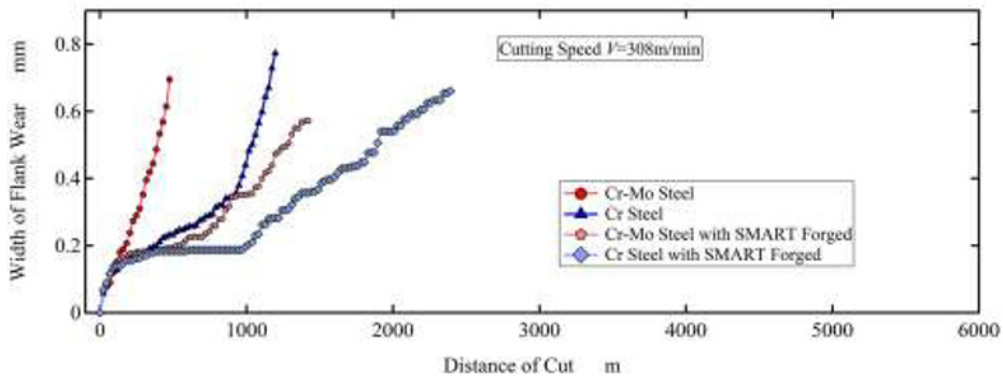

(d) Cutting speed *V*=308m/min

Fig. 7. Relationship between distance of cut and width of flank wear

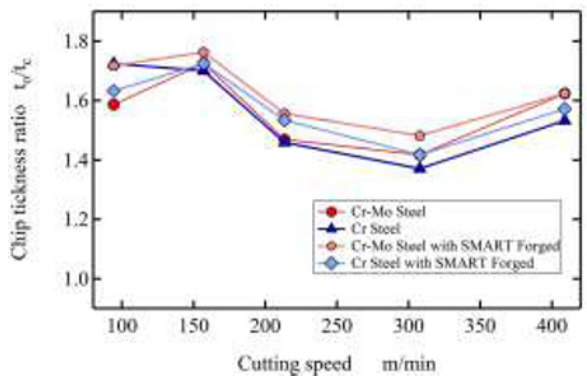

Fig. 8. Relationship between cutting speed and chip thickness ratio

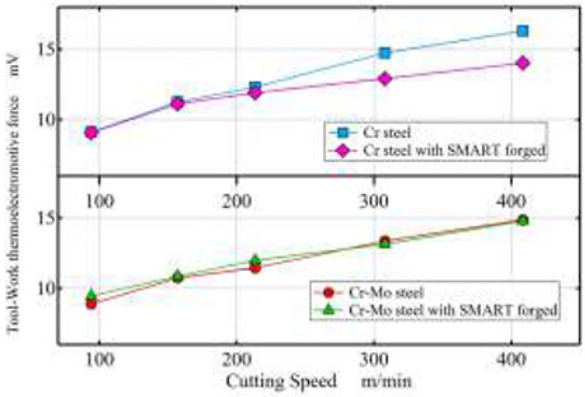

Fig. 10. Relationship between cutting speed and Tool-work thermoelectromotive force

Next, the microscope observation of the chip surface to be discharged and the cutting temperature at that time were investigated. Figure 9 shows the photographs of the chips discharged from chromium molybdenum steel made by SMART forging process classified according to the cutting speed. From these photographs, it can be seen that the pluck type chip is discharged up to the cutting speed V of V=157 m/min, and it is changed to the flow type chip at the cutting speed V of V=213 m/min or more. That is, it can be seen that the chip thickness ratio shown in fig. 8 and the chip configuration show a very good relationship. This tendency was almost the same for the other three materials.

The cutting temperature at that time is shown in fig.10. It can be seen that the cutting temperature increases in proportion to the rise in the cutting speed in both materials. From these results, it is considered that built-up edges are generated because the cutting temperature is close to the recrystallization temperature of the workpiece at a cutting speed V of V=157 m/min or less regardless of which material is cut. And the breakage of the cutting edge occurs due to the separation of the built-up edges. However, with respect to the cutting temperature, only relative comparison is made for each material. From now on, it is necessary to fabricate a thermocouple of cemented carbide and each forged material and investigate the absolute temperature during cutting while calibrating the temperature.

From the above, it can be considered that in the cutting of these forged materials, the occurrence of the built-up edges is remarkable near the recrystallization temperature of the material, which causes the tool to be frequently chipped. Therefore, when cutting these forged materials with cemented carbide, it is necessary to cut at a cutting speed V of V=213 m/min or more. However, when cutting at the cutting speed V of V=308 m/min, tool life becomes extremely short, so it is considered that the optimum cutting condition per cutting speed V of V=213 m/min.

4 Conclusion

In order to investigate the machinability of the material made by the new forging method, we examined the cutting speed region which could not be covered in the previous report. As the result, it was found that general cutting speeds such as cutting the steel with cemented carbide are not suitable for cutting conditions of these forged materials because the tool frequently chip. For this reason, the chip thickness ratio the microscope

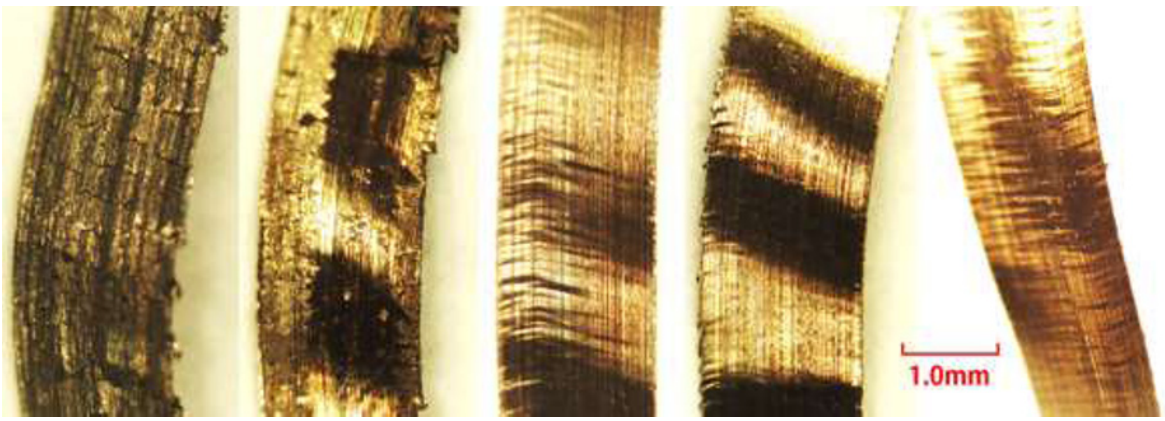

V=94.2m/min V=157m/min V=213m/min V=308m/min V=409m/min

Fig. 9. Photograph of the chips surface at each cutting speed.

observation of the chip surface and the cutting temperature were measured. As a result, at the cutting speed V of V=157 m/min or less, it reached the conclusion that the built-up edges frequently occurred and the tool was chipped due to it. From the previous report and the results of this experiment, it was found that the cutting speed V of about V=213 m/min is optimum for cutting these forged materials with cemented carbide.

The materials used in this experiment are finally gear cutting processed. Therefore, from now on, it is necessary to study machinability including tool life by using fly tool made by coated high speed steel. In addition, we will also clarify the cause of the difference in tool life observed by the difference in the heat treatment after forging which was reported in the previous report.

I am thankful to **Kawakami Ironworks Co., Ltd**., who provided materials for the performance of this experiment. (http://www.kawakami-ironworks.com/)

References

1. Murata M., Hino M., Kuwano R. and Kurokawa S., (2018). Machinability of SMART Forged Materials in Intermittent Cutting, International Journal of Materials Science and Engineering, 6, No.1, 1-9
2. Uchida K., Hino M., et al. (2017). Material Control Technology for Gear Shaft Forged Products with TMCP (SMART Forging Process) (1st Report), Journal of JFA, Japan, No.58, 77-86, (in Japanese)
3. Uchida K., Hino M., et al. (2017). Material Control Technology for Gear Shaft Forged Products with TMCP (SMART Forging Process) (2nd Report), Journal of JFA, Japan, No.59, 114-126, (in Japanese)
4. Murata M., Kurokawa S., Ohnishi O., Doi T. and Uneda M. (2011). Characteristics of Thermo-electromotive Force, Electric Current and Electric Resistance in Intermittent Cutting Process by Face Milling, Advanced Materials Research, 314-316, 1075-1078.
5. Murata M., Kurokawa S., Ohnishi O., Uneda M., Doi T., (2012). Real-Time Evaluation of Tool Flank Wear by In-Process Contact Resistance Measurement in Face Milling, Journal of Advanced Mechanical Design, Systems, and Manufacturing, 6, No.6, 958-970.
6. Hirota H., Suzuki S., Shinozaki N. (1979). The Correlation between Chip Breaking and Tool-work Thermo-electromotive, Journal of the Japan Society for Precision Engineering, Japan, 45, No.8, 39-45, (in Japanese)
7. Hirota H., Suzuki S., Shinozaki N. (1979). Fluctuating Characteristics of Tool-work Thermo-electromotive Force, Journal of the Japan Society for Precision Engineering, Japan, 45, No.5, 68-74, (in Japanese)